Aluminum-Titanium Complex Deoxidation Equilibria in Fe-Cr-Al-Ti-O Melts

MIN-KYU PAEK, JUNG-MOCK JANG, JONG-OH JO, LAURI HOLAPPA, and JONG-JIN PAK

Al-Ti complex deoxidation equilibria in high Cr stainless steels were studied by measuring the thermodynamic behavior of O in the Fe-Cr-Al-O, Fe-Cr-Ti-O, and Fe-Cr-Al-Ti-O melts. The present deoxidation experiments were thermodynamically analyzed along with available data in the literature using Wagner's formalism. The compatible set of parameters for the multicomponent Fe-Cr-Al-Ti-O system was selected, and its applicable concentration and temperature limits were discussed. The parameter set successfully reproduced the present experimental results and literature data of deoxidation equilibria in the Fe-Cr-Al-O and Fe-Cr-Ti-O alloy melts over the wide Cr concentration up to 40 mass pct at 1823 K to 1996 K (1550 °C to 1723 °C). The validity of the parameters was also checked by carrying out the Al-Ti complex deoxidation experiments with the construction of the predominance diagram for inclusions in the Fe-Cr-Al-Ti-O melts at 1873 K (1600 °C).

I. INTRODUCTION

ALUMINUM and titanium are both important alloying elements for the refining process of ferritic stainless steels and the physical properties of the final products. Al is added after the decarburization process of stainless steelmaking to deoxidize the liquid steel as well as to recover Cr by reducing the remaining Cr_2O_3 in the converter slag. The main purpose of Ti alloying in ferritic stainless steels is "stabilization." When the Ti content exceeds the critical amount (e.g., [pct Ti] = 0.2 + 4 ([pct C] + [pct N])), it binds effectively the dissolved C and N by forming TiC and TiN precipitates in solid steel. The formation of Cr carbides and nitrides is then avoided.[1] Adding Ti following Al deoxidation is effective in minimizing excess oxidation of Ti and enhance the corrosion resistance by the improved yield of Ti, while the formation of Ti oxide inclusions cannot be completely avoided due to its relatively high affinity with O in the liquid steel. Since the various kinds of deoxidation products such as Al_2O_3, Ti_3O_5, and Ti_2O_3 can be coexisting in the steel melt, these simultaneous reactions have been called "Al-Ti complex deoxidation equilibria" in liquid iron alloys. The Al-Ti complex deoxidation in liquid iron has been extensively studied from various points of view; inclusion evolution,[2,3] inclusion morphology and chemistry,[4–8] inclusion stability diagram,[9–11] refractory corrosion,[12] clogging of submerged entry nozzle,[13,14] re-oxidation,[15] and grain refinement.[16] However, the fundamental studies on the Al-Ti complex deoxidation equilibria in the Cr containing liquid steel are very scarce.

To understand the various phenomena during the Al-Ti complex deoxidation in ferritic stainless steel melts, accurate thermodynamic information on O behavior and oxide formation in Fe-Cr-Al-Ti-O alloy melts has to be secured first. Therefore, in the present study, the Al and Ti deoxidation equilibria in Fe-Cr alloy melts were measured at 1823 K to 1923 K (1550 °C to 1650 °C) by the addition of the deoxidizers. Wagner's formalism[17] was used to analyze the present experimental results and the available literature data. Although there are inherent limitations of the interaction parameter formalism to describe the thermodynamics of O in the entire alloy concentration,[18] it is practically acceptable for the composition range of commercial ferritic stainless steels containing Al and Ti up to 0.2 and 0.8 mass pct, respectively. The consistent set of interaction parameters and the equilibrium constants for the oxide formation reactions in liquid iron were selected from the authors' recent studies[19–23] and reported values[24–26] for the multicomponent

MIN-KYU PAEK and LAURI HOLAPPA are with the Department of Chemical and Metallurgical Engineering, Aalto University, Espoo, 02150, Finland; JUNG-MOCK JANG is with the Steelmaking Research Group, Technical Research Lab., POSCO, Pohang, 37859, Korea; JONG-OH JO is with the R&D Center, Hyundai Steel Co. Ltd, Dangjin, 31719, Korea; JONG-JIN PAK is with the Department of Materials Science and Chemical Engineering, Hanyang University, ERICA, Ansan, 15588, Korea. Contact e-mail: jjpak@hanyang.ac.kr

Fe-Cr-Al-Ti-O alloy system as listed in Table I. The validity of the parameters was checked by carrying out the Al-Ti complex deoxidation experiments with the construction of the inclusion predominance diagrams for the Fe-Cr-Al-Ti-O melts at 1873 K (1600 °C).

II. EXPERIMENTAL PROCEDURES

A. Measurement of Al-O Relation in Fe-Cr Melt

The Al-O relation was measured in Fe-Cr melt in equilibrium with pure solid Al_2O_3 at 1873 K (1600 °C). Four hundred grams of electrolytic Fe (99.99 pct purity) and Cr (99.99 pct purity) charged in an Al_2O_3 crucible (outer diameter (OD): 56 mm, inner diameter (ID): 50 mm, height (H): 96 mm) were melted using a 15 kW/30 kHz high-frequency induction furnace. In order to minimize the excessive formation of oxide inclusions, the initial O content in the melt was forcibly controlled below 40 mass ppm by blowing Ar-10 vol pct H_2 gas onto the melt surface at a high flow rate of 2 L/min for 4 hours. The melt temperature was directly measured by immersing the R-type (Pt/Pt: 13 mass pct Rh) thermo-couple sheathed with the closed one-end Al_2O_3 tube (OD: 6 mm). The temperature was accurately controlled within 2 °C by a proportional-integral-derivative (PID) controller. Then, the gas was switched to the dehydrated and deoxidized Ar gas. In order to purify the Ar gas, the high-purity Ar (purity level 6) was passed through the silica gel and phosphorus pentoxide to remove the moisture and then blown into the pre-heating resistance furnace charged with the sponge Ti (99.9 pct purity). The Ti turning furnace was heated up to 1173 K (900 °C) for the best oxidation condition of Ti for consuming the oxygen in the Ar gas. The gas flow rate was adjusted

Table I. Thermodynamic Parameters of Alloying Elements in Liquid Iron Used in the Present Study

System	Interaction Parameter	Value (1873 K (1600 °C))	Temp. (K), [pct i] Range	References
Fe-O	e_O^O	$-1750/T + 0.76\ (-0.17)$	1823 to 1923, [pct O] < 0.2	25
	r_O^O	0		
Fe-Al-O	e_{Al}^{Al}	0.043	1823 to 1973, [pct Al] < 4.5	19
	r_{Al}^{Al}	0		
	e_O^{Al}	(-1.17)	1873 to 1973, [pct Al] < 2.53	24
	r_O^{Al}	0		
	e_{Al}^O	(-1.98)		
	r_{Al}^O	0		
	$\log K_{Al_2O_3}$	$-64{,}000/T + 20.57\ (-13.6)$		
Fe-Ti-O	e_{Ti}^{Ti}	0.048	1823 to 1973, [pct Ti] < 0.52	20
	r_{Ti}^{Ti}	0		
	e_O^{Ti}	$-1642/T + 0.3358\ (-0.541)$	1823 to 1923, [pct Ti] < 4.75	23
	r_O^{Ti}	0.0385		
	e_{Ti}^O	$-4915/T + 1.005\ (-1.62)$		
	r_{Ti}^O	-0.355		
	$\log K_{Ti_3O_5}$	$-72{,}813/T + 21.32$ (-17.56)		
	$\log K_{Ti_2O_3}$	$-44{,}238/T + 13.0\ (-10.62)$		
Fe-Cr-O	e_O^{Cr}	$-123/T + 0.034\ (-0.032)$	1823 to 1923, [pct Cr] < 46	26
	r_O^{Cr}	0		
	e_{Cr}^{Cr}	0		
	r_{Cr}^{Cr}	0		
Fe-Al-Ti-O	$r_O^{Al,Ti}$	0	1873, [pct Al] < 0.03, [pct Ti] < 0.59	Present study
	e_{Al}^{Ti}	-0.011	1823, [pct Al] < 2, [pct Ti] < 0.14	21
	r_{Al}^{Ti}	0		
	e_{Ti}^{Al}	-0.024	1823 to 1973, [pct Al] < 1.6, [pct Ti] < 0.55	
	r_{Ti}^{Al}	0		
Fe-Cr-Al-O	$r_O^{Cr,Al}$	0	1873, [pct Cr] < 16, [pct Al] < 0.81	Present study
	e_{Al}^{Cr}	0.017	1823 to 1973, [pct Cr] < 26, [pct Al] < 3.2	21
	r_{Al}^{Cr}	0		
Fe-Cr-Ti-O	$r_O^{Cr,Ti}$	0	1873, [pct Cr] < 16, [pct Ti] < 0.98	Present study
	e_{Ti}^{Cr}	$406.7/T - 0.1933\ (0.024)$	1823 to 1923, [pct Cr] < 30, [pct Ti] < 1.5	22
	r_{Ti}^{Cr}	$-20.6/T + 0.011\ (0)$		

to 0.5 L/min. The Al-O relation in Fe-Cr melt was measured with the addition of Al shot (99.99 pct purity). Each equilibration took 2 hours, which was confirmed by the sampling and subsequent analysis of the O content at 30 min intervals. The addition of Al was repeated up to 1 mass pct relative to the total weight of melt.

B. *Measurement of Ti-O Relation in Fe-Cr Melt*

Prior to the Ti deoxidation experiments, the high-purity electrolytic Fe and Cr were pre-melted for the target composition of Fe-18 mass pct Cr under the Ar-10 vol pct H_2 gas atmosphere. The Ti-O relation in the pre-melted Fe-Cr alloy was measured at 1823 K to 1923 K (1550 °C to 1650 °C). In order to obtain the equilibrium data under the Ti_2O_3 stable region, the Ti_2O_3 lined alumina crucible (OD: 40 mm, ID: 30 mm, H: 50 mm) was used. The smaller size of the crucible than the Al deoxidation experiment was used for keeping the thin inner layer made of Ti_2O_3 powder on the crucible wall. Thus, a smaller amount of Fe-Cr alloy was charged in the crucible. One hundred grams of the alloy were melted under the purified Ar atmosphere. After melting, the first Ti shot (99.9 pct purity) was added for 0.5 mass pct Ti of the target composition where the melt can be equilibrated with Ti_2O_3. The melt was equilibrated for 2 hours, and a metal sample was extracted by quartz tube. Depending on the Ti oxide lining condition with the well-preserved inner wall of Ti oxide, the second Ti shot was added to reach the higher target content of 1 mass pct Ti in Fe-Cr melt.

C. *Measurement of Complex Deoxidation in Fe-Cr-Al-Ti Melt*

In order to study Al-Ti complex deoxidation equilibria under the coexisting condition of Al_2O_3 and Ti_3O_5, one hundred grams of Fe-18 mass pct Cr alloy was melted and deoxidized by the simultaneous additions of Al and Ti under the purified Ar atmosphere at 1873 K (1600 °C). Three separate experiments were carried out depending on the Al and Ti concentration in the Fe-Cr melt. The alloy melt was equilibrated with the alumina wall of the smaller crucible (OD: 40 mm, ID: 30 mm, H: 50 mm) as well as the bottom layer of Ti_3O_5 powder. By applying strong pressure for charging Ti_3O_5 powder, it was possible to keep the initial position of the bottom layer without floatation. After 2 hours of equilibration, the melt was quenched rapidly by blowing helium gas onto the melt surface.

D. *Sampling and Analysis*

The quenched samples were sectioned for the chemical analysis and polished to remove the oxide layer formed on the surface. The total O content of the metal samples was measured by the inert gas fusion-infrared absorptiometry technique using the nitrogen/oxygen analyzer (LECO TC-600). The concentration of metallic elements such as Al, Ti, and Cr in the metal samples was analyzed by the Inductively Coupled Plasma-Atomic Emission Spectroscopy (ICP-AES, SPECTRO ARCOS). The

oxide layer formed on the top of the melt surface was characterized by the electron backscatter diffraction (EBSD) pattern for the identification of the equilibrium oxide phase. In parallel, the oxide inclusions suspended inside the melt were extracted from the metal sample by the potentiostatic electrolytic technique.[27] The inclusion morphology and composition were analyzed by the Scanning Electron Microscopy-Energy Dispersive X-ray Spectroscopy (SEM-EDS, Hitachi S4800).

III. RESULTS AND DISCUSSION

A. *Al Deoxidation Equilibria in Fe-Cr Alloy Melt*

The Al deoxidation equilibria in liquid iron can be represented by the dissolved Al and O contents in liquid iron in equilibrium with solid Al_2O_3. The contour of the equilibrium relation between Al and O in liquid iron gives the Al deoxidation curve, which also means the liquidus line of solid Al_2O_3 in the Fe-Al-O ternary system. A comprehensive review of experimental techniques and theoretical studies of Al deoxidation equilibria in liquid iron was reported elsewhere.[28] Among the previous studies, the result of Rohde et al.[24] has been widely used as a recommended value, for instance, by the Japan Society for the Promotion of Science (JSPS).[29] Even though their result is applicable only for the low Al concentration region,[18] it is valid for the typical Al killed steels and ferritic stainless steels.

The Al deoxidation equilibrium in liquid iron can be expressed by the following equilibrium reaction for the dissolution of pure solid Al_2O_3 in liquid iron[24]:

$$Al_2O_3(s) = 2\underline{Al} + 3\underline{O} \quad [1]$$
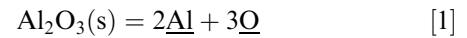
$$\Delta G_1^\circ = 1,225,000 - 393.8T \text{ J/mol} \quad [2]$$

$$K_1 = \frac{h_{Al}^2 h_O^3}{a_{Al_2O_3}} = \frac{f_{Al}^2 f_O^3 [\text{pct Al}]^2 [\text{pct O}]^3}{a_{Al_2O_3}}, \quad [3]$$

where K_1, $a_{Al_2O_3}$, h_i, f_i, and [pct i] are the equilibrium constant, the activity of Al_2O_3, the Henrian activity, Henrian activity coefficient, and the equilibrium concentration of i in mass pct, respectively. The value of log K_1 = − 64,000/T + 20.57 determined by Rohde et al.[24] was adopted in this study. $a_{Al_2O_3}$ was set to unity.

In a Fe-Cr-Al-O multicomponent alloy melt, the activity coefficient of Al and O, f_{Al} and f_O can be expressed as the following relation using only first-order interaction parameters by Wagner's formalism[17]:

$$\log f_{Al} = e_{Al}^O[\text{pct O}] + e_{Al}^{Al}[\text{pct Al}] + e_{Al}^{Cr}[\text{pct Cr}] \quad [4]$$

$$\log f_O = e_O^O[\text{pct O}] + e_O^{Al}[\text{pct Al}] + e_O^{Cr}[\text{pct Cr}], \quad [5]$$

where e_i^j is the first-order interaction parameter of j on i in liquid iron in mass pct.
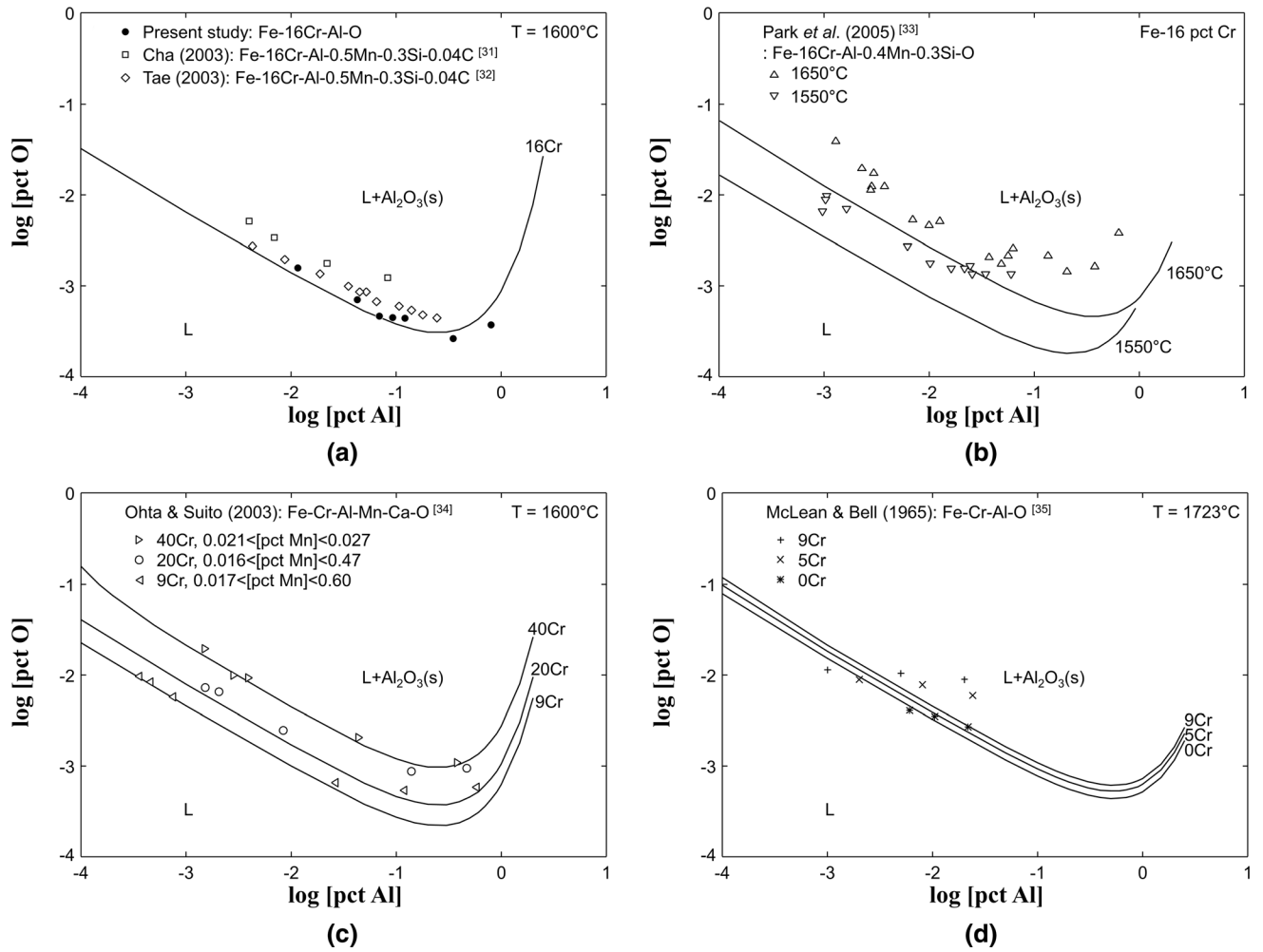
Fig. 1—Al deoxidation equilibria (*a*) in Fe-16 pct Cr at 1873 K (1600 °C), (*b*) 1823 K and 1923 K (1550 °C and 1650 °C), (*c*) in Fe-9, 20, 40 pct Cr at 1873 K (1600 °C), and (*d*) in Fe-0, 5, 9 pct Cr at 1996 K (1723 °C).

The self-interaction parameter of O, e_O^O and the interaction parameters between Al and O, e_O^{Al} and e_{Al}^O in liquid iron were taken from the recommended values in JSPS.[24,25,29] The value of e_O^{Cr} measured under the unit activity of Cr_2O_3 by Itoh *et al.*[26] was adopted in the present study rather than the value measured by Nakamura and Uchimura[30] using MgO crucible coated by $MgO \cdot Cr_2O_3$ powder (recommended value of JSPS).[29] In the authors' recent studies,[19,21] the e_{Al}^{Cr} and e_{Al}^{Cr} values have been determined from the stable solubility product data of AlN formation, respectively, in Fe-Al-N and Fe-Cr-Al-N alloy melt under the unit activity of AlN by the metal/nitride/gas equilibration technique. As mentioned in the author's previous study,[21] it is very difficult to measure the specific effect of Cr on Al in liquid iron by the deoxidation experiment due to the big scattering of measured equilibrium O contents by the formation of secondary oxide inclusions during quenching and solidification. Therefore, the e_{Al}^{Al} and e_{Al}^{Cr} values determined by the metal/nitride/gas equilibration technique were adopted in the present study. All the interaction parameters used in the present study are summarized in Table I. The second-order parameters were assumed negligible in the Fe-Cr-Al-O system, and Eqs. [[4]] and [[5]] were only expressed with the first-order interaction parameters.

Using the thermodynamic parameters mentioned above, the Al-O relations in Fe-Cr alloy melts at the various Cr concentration and temperatures were calculated as shown in Figure 1. The Al deoxidation equilibria in Fe-Cr alloy melt have been measured by several researchers.[31–35] However, most studies have been carried out in the practical ferritic stainless steels containing other alloying elements or impurities such as Mn, Si, Ni, Ca, Mg, and C. Therefore, in the present study, the Al deoxidation equilibria in Fe-16 mass pct Cr melt were measured over the wide Al concentration range up to 0.81 mass pct at the typical steelmaking temperature of 1873 K (1600 °C) using the high-purity raw materials. As shown in Figure 1(a), the present experimental results corresponded very well with the calculated Al-O relation in Fe-16 mass pct Cr melt up to 0.81 mass pct Al by using the first-order interaction parameters. No additional second-order cross-product parameter was required for the description of O
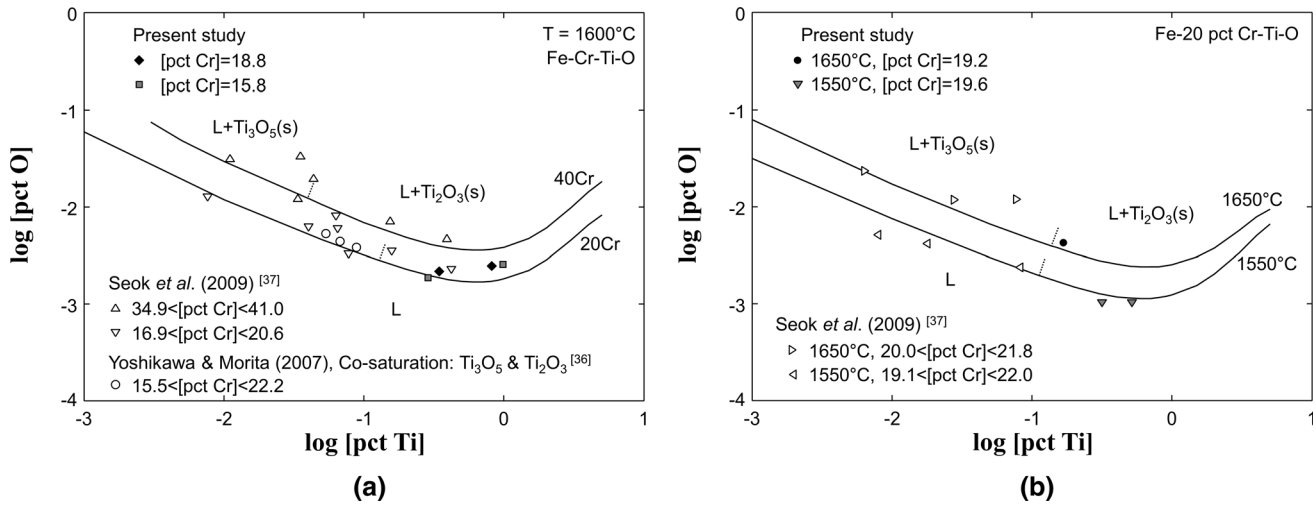
Fig. 2—Ti deoxidation equilibria in Fe-Cr melt at (a) 1873 K (1600 °C) and (b) 1823 K and 1923 K (1550 °C and 1650 °C).

behavior in the Fe-Cr-Al-O system such as the simultaneous effect of Cr and Al on the O content in liquid iron, $r_O^{Cr,Al}$.

Cha[31] measured the Al deoxidation equilibria in Fe-16 mass pct Cr-0.5 mass pct Mn-0.3 mass pct Si-0.04 mass pct C melt at 1873 K (1600 °C) with the addition of Al and Ni-10 mass pct Mg alloys as deoxidizers for the research of the MgO·Al₂O₃ spinel formation in 430 stainless steel. Tae[32] measured the Al deoxidation using the same commercial ferritic stainless steel with Cha,[31] and added Ni-10 mass pct Ca alloy and CaO-Al₂O₃ slag into the melt to check the Ca treatment effect. However, their O contents were slightly higher than the present experimental results and prediction at the same Cr content and temperature as can be seen in Figure 1(a). Park et al.[33] also carried out the Al deoxidation equilibria in the commercial stainless steel containing 0.4 mass pct Mn and 0.3 mass pct Si, respectively. Additionally, they successfully investigated the mechanism of inclusion formation by the addition of CaSi₂ in the melt. As shown in Figure 1(b), their deoxidation results were also higher than the calculated deoxidation curve by the present study in Fe-16 mass pct Cr at 1823 K and 1923 K (1550 °C and 1650 °C). It may seem to need further researches of the alloying (Ni-Mg,[31] Ni-Ca,[32] CaSi₂ alloy,[33] and Mn), slag (MgO-Al₂O₃[31] and CaO-SiO₂ system[32,33]), and cleanliness (initial O content and impurity level) on the deoxidation equilibria in Fe-Cr alloy melts. Ohta and Suito[34] measured not only Al deoxidation equilibria in Fe-Cr melts containing 9, 20, and 40 mass pct Cr but also the Mn distribution at 1873 K (1600 °C) by the equilibrium between CaO-Al₂O₃ slag and Fe-Cr-Al-Mn melt. Even though their alloy contained Mn up to 0.6 mass pct, the Al-O relation plotted using their total Al and O contents corresponded very well with the present calculation at low Al concentration as shown in Figure 1(c). Among the previous studies, only McLean and Bell[35] measured the Al deoxidation equilibria in the Fe-Cr-Al-O system without any other alloying elements and impurities under the controlled O potential by the H₂/H₂O gas

mixture. However, they carried out the equilibrium experiments in the limited Cr and Al concentration ranges, [pct Cr]<9.3 and [pct Al]<0.024 and temperature, 1996 K (1723 °C). As shown in Figure 1(d), the present calculation corresponded well only with their data without Cr addition.

B. Ti Deoxidation Equilibria in Fe-Cr Alloy Melt

There is a phase transition of the equilibrium Ti oxide depending on the Ti concentration in liquid iron and the corresponding equilibrium O partial pressure because of the multiple oxidation states of Ti (Ti^{2+}, Ti^{3+}, and Ti^{4+}). That is, various equilibrium reactions have to be considered to understand the Ti deoxidation equilibria in liquid iron alloys. In the commercial-grade of Ti containing steel melts, typical equilibrium oxide phases are Ti_3O_5 and Ti_2O_3.[23]

The Ti deoxidation equilibria in liquid iron can be expressed by the following equilibrium reactions for the dissolution of pure solid Ti_3O_5 and Ti_2O_3 in liquid iron[23]:

$$Ti_3O_5(s) = 3\underline{Ti} + 5\underline{O} \qquad [6]$$
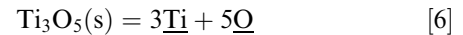
$$\Delta G_6^\circ = 1,392,344 - 407.7T \text{ J/mol} \qquad [7]$$

$$K_6 = \frac{h_{Ti}^3 h_O^5}{a_{Ti_3O_5}} = \frac{f_{Ti}^3 f_O^5 [\text{pct Ti}]^3 [\text{pct O}]^5}{a_{Ti_3O_5}} \qquad [8]$$

$$Ti_2O_3(s) = 2\underline{Ti} + 3\underline{O} \qquad [9]$$

$$\Delta G_9^\circ = 845,928 - 248.6T \text{ J/mol} \qquad [10]$$

$$K_9 = \frac{h_{Ti}^2 h_O^3}{a_{Ti_2O_3}} = \frac{f_{Ti}^2 f_O^3 [\text{pct Ti}]^2 [\text{pct O}]^3}{a_{Ti_2O_3}}. \qquad [11]$$

In a Fe-Cr-Ti-O multicomponent alloy melt, the activity coefficients of Ti and O, f_{Ti} and f_O can be expressed as the following relations using Wagner's formalism:[17]

$$\log f_{Ti} = e_{Ti}^O [\text{pct O}] + r_{Ti}^O [\text{pct O}]^2 + e_{Ti}^{Ti} [\text{pct Ti}]$$
$$+ e_{Ti}^{Cr} [\text{pct Cr}] + r_{Ti}^{Cr} [\text{pct Cr}]^2 \qquad [12]$$

$$\log f_O = e_O^O [\text{pct O}] + e_O^{Ti} [\text{pct Ti}]$$
$$+ r_O^{Ti} [\text{pct Ti}]^2 + e_O^{Cr} [\text{pct Cr}], \qquad [13]$$

where r_i^j is the second-order interaction parameter of j on i in liquid iron in mass pct.

In the authors' recent study,[23] the first- and second-order interaction parameters between Ti and O in liquid iron (e_{Ti}^O, r_{Ti}^O, e_O^{Ti}, and r_O^{Ti}) and the equilibrium constants of Reactions [6] and [9] (log $K_6 = -72,813/T + 21.32$ and log $K_9 = -44,238/T + 13.0$) were simultaneously determined by the Ti deoxidation experiments in liquid iron at 1823 K to 1923 K (1550 °C to 1650 °C). Compared to the Al-O interaction in liquid iron, the Ti-O interaction was less negative in liquid iron. Thus, the Ti-O relation has been described up to the higher alloying concentration of 4.75 mass pct Ti by introducing the second-order interaction parameters, r_{Ti}^O and r_O^{Ti} without any mathematical failure of the formalism such as multi-extrema (minimum and maximum) on the Ti deoxidation curve. The specific effects of alloying elements on Ti in liquid iron have also been determined by another method of the metal/nitride/gas equilibration technique.[20,22] The self-interaction parameter of Ti, e_{Ti}^{Ti} and the effect of Cr on Ti, e_{Ti}^{Cr}, and r_{Ti}^{Cr} in liquid iron have been determined under the stable TiN saturation condition. As discussed in the preceding section, such essential parameters determined in the authors' rece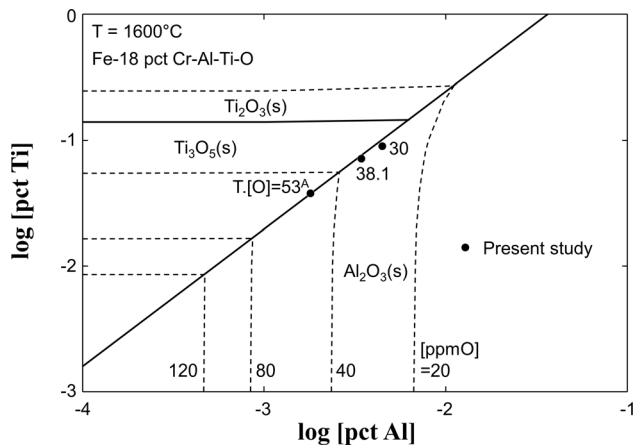nt studies[20,22,23] under the unit activity of nitride were adopted in this study for the multicomponent Fe-Cr-Ti-O alloy melt. The interaction parameters used for the Fe-Cr-Ti-O system are also listed in Table I.

Using Eqs. [6] through [13] with the selected interaction parameters, the Ti-O relations in Fe-Cr melts at various Cr concentration and temperatures were calculated as shown in Figure 2. In the Fe-Cr-Ti-O system, a few studies of the Ti deoxidation equilibria in liquid Fe-Cr alloy have been reported.[36,37] Yoshikawa and Morita[36] measured the critical Ti and O contents in Fe-Cr melt at the co-saturation point of Ti_3O_5 and Ti_2O_3. They measured the critical composition over the wide Cr concentration range from 0.6 to 30.9 mass pct under the purified Ar atmosphere at 1873 K (1600 °C) using the Ti oxide crucible consisting of the mixture of Ti_3O_5 and Ti_2O_3. Their data in the Cr range from 15.5 to 22.2 mass pct were plotted together with the present calculation for the Fe-20 and 40 mass pct Cr melt as shown in Figure 2(a). By increasing Cr content, the O content increased, whereas their critical Ti content decreased shown as open circles in Figure 2(a). The decreasing trend of equilibrium Ti content with increasing Cr content in their experimental results agreed with the present calculation, however, their Ti concentration at the critical point of co-saturation was much lower than the calculated three-phase univariant of the Fe-20 mass pct Cr melt, Ti_3O_5, and Ti_2O_3 marked on the deoxidation curves by dotted lines. As shown in Figures 2(a) and (b), Seok et al.[37] measured the Ti-O relation over a wider range of Cr content from 16.9 to 41.0 mass pct at 1823 K to 1923 K (1550 °C to 1650 °C). Most of their results were measured at the limited Ti concentration range under the Ti_3O_5 saturation; moreover, it was significantly scattered at low Ti concentration in Fe-Cr melt. The huge scattering of O analysis at low Ti range can be caused by several reasons; (i) a lack of O source to take part in the deoxidation equilibria to reach a high equilibrium O content at low Ti region in the Ti_3O_5 saturation condition, (ii) the decrease of $a_{Ti_3O_5}$ by the solid solubility of Fe or Cr in the pseudobrookite phase, and (iii) the formation of complex oxide phases such as liquid oxide.[14] To avoid such errors, in this study, the Ti deoxidation equilibria in Fe-Cr alloy melt were measured at the relatively higher Ti concentration region under the Ti_2O_3 saturation in the temperature

Fig. 3—Calculated inclusion predominance diagram for Fe-18 pass pct Cr-Al-Ti-O system at 1873 K (1600 °C) with the present experimental results.
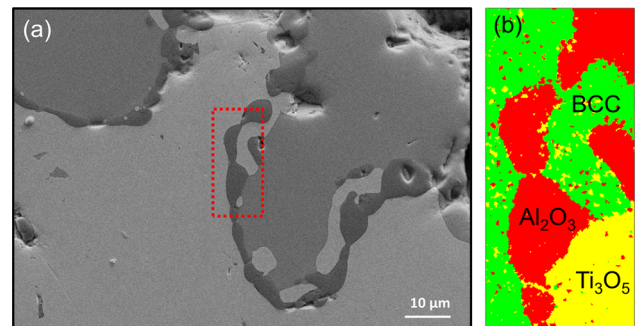

Fig. 4—(a) SEM image of formed oxide near the melt surface of sample 'A' and (b) EBSD analysis of the enlarged part of the square box in (a).

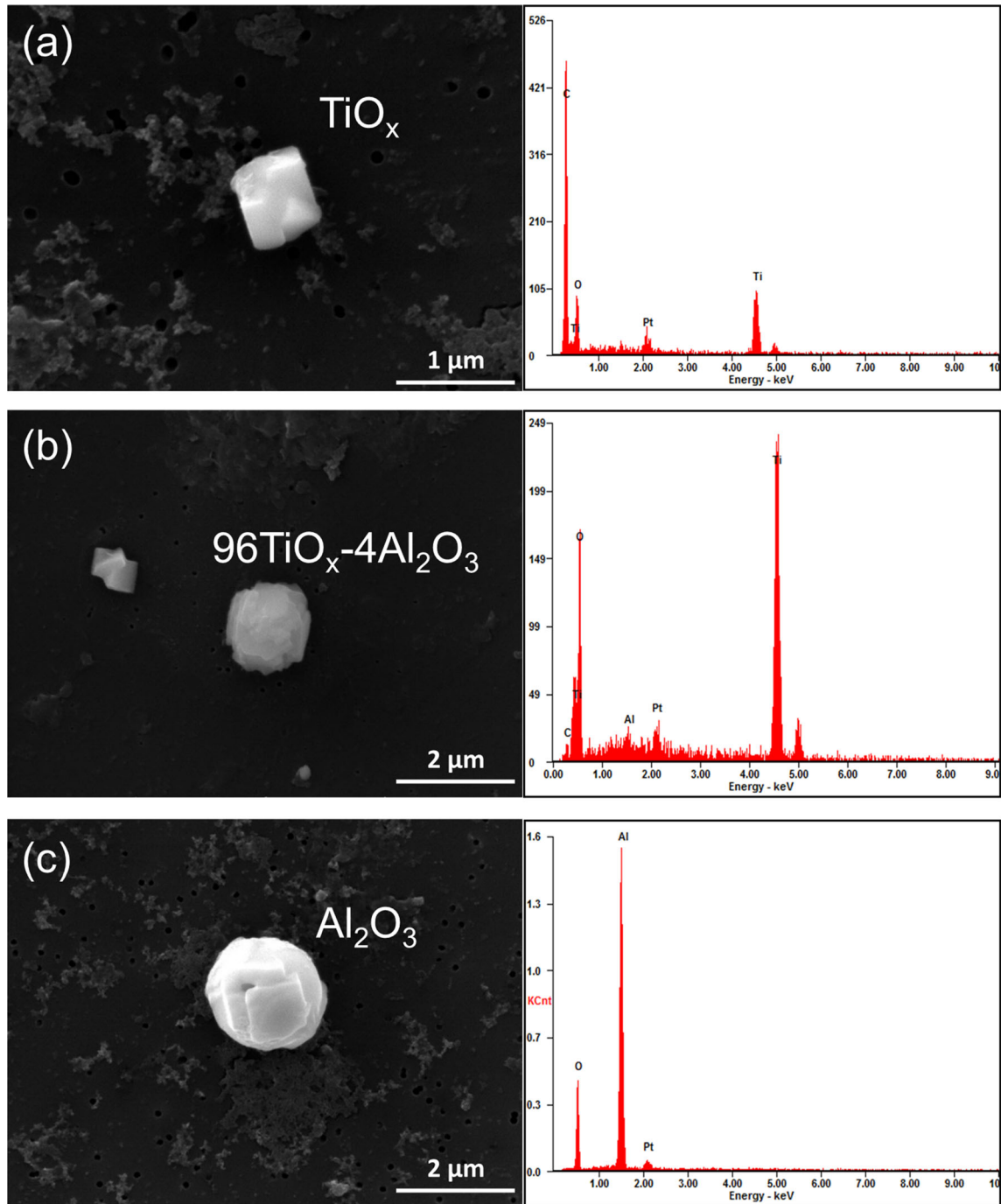Fig. 5—SEM images and EDS analysis of extracted inclusions in sample 'A': (a) Ti oxide, (b) Ti-rich TiO_x-Al_2O_3 inclusion, and (c) Al_2O_3.

range from 1823 K to 1923 K (1550 °C to 1650 °C). The present experimental results correlated well with the calculated deoxidation curves and the previous data measured at lower Ti contents. Like the Fe-Cr-Al-O system, no additional second-order cross-product parameter of Cr and Ti on O in liquid iron, $r_O^{Cr,Ti}$, was required for the description of O behavior in the Fe-Cr-Ti-O melt containing Ti up to 0.98 mass pct at 1823 K to 1923 K (1550 °C to 1650 °C).
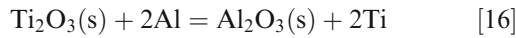
C. Al-Ti Complex Deoxidation in Liquid Fe and Fe-Cr Alloy

When Al and Ti coexist as deoxidizers in liquid iron alloys, the equilibrium oxide phase can be Al_2O_3, Ti_2O_3, or Ti_3O_5 depending on the Al, Ti, and Cr contents. Figure 3 shows the inclusion predominance diagrams for Fe-18 mass pct Cr-Al-Ti-O melts constructed using all thermodynamic parameters listed in Table I. The dashed lines represent the contours of the iso-oxygen
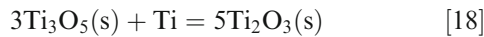
content in the melt. The boundary lines among Al_2O_3, Ti_3O_5, and Ti_2O_3 can be calculated from Eq. [2], [7], and [10]. The Gibbs free energy changes of the boundary reactions were derived as

$$3Ti_3O_5(s) + 10Al = 5Al_2O_3(s) + 9Ti \qquad [14]$$
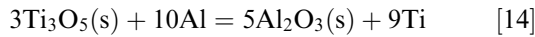
$$\Delta G^{\circ}_{14} = -1,947,968 + 745.9T \text{ J/mol} \qquad [15]$$

$$Ti_2O_3(s) + 2Al = Al_2O_3(s) + 2Ti \qquad [16]$$

$$\Delta G^{\circ}_{16} = -379,072 + 145.2T \text{ J/mol} \qquad [17]$$

$$3Ti_3O_5(s) + Ti = 5Ti_2O_3(s) \qquad [18]$$

$$\Delta G^{\circ}_{18} = -52,608 + 19.9T \text{ J/mol}. \qquad [19]$$

The activities of Al_2O_3, Ti_3O_5, and Ti_2O_3 can be considered as unity due to the limited mutual solubility within the Al and Ti concentration range of Figure 3. The Fe or Cr dissolution in the oxide phases by the oxidation was negligible under the strong reducing condition. The interactions between Al and Ti in liquid iron, e^{Al}_{Ti} and e^{Ti}_{Al}, determined by the nitride equilibration technique[21] were additionally considered for the activity coefficient of Al and Ti in the Fe-Cr-Al-Ti-O melts. The second-order cross-product parameter of Al and Ti on O in liquid iron, $r^{Al,Ti}_{O}$, was also assumed to be zero in the multicomponent system.

In order to check the validity of the thermodynamic parameters, Al-Ti complex deoxidation experiments were carried out under the co-saturation of Al_2O_3 and Ti_3O_5 in the Fe-18 mass pct Cr melts at 1873 K (1600 °C). As shown in Figure 3, the Al and Ti contents in Fe-18 mass pct Cr alloy were located well on the boundary line where the pure solid Al_2O_3 and Ti_3O_5 coexist. The measured equilibrium O contents at the co-saturated condition correlate very well with the calculated iso-oxygen contours. As shown in Figure 4, the coexistence of Al_2O_3 and Ti_3O_5 phases was confirmed by the EBSD analysis of oxide layers in contact with the Fe-18 mass pct Cr melt containing 0.0018 mass pct Al, 0.038 mass pct Ti, and 53 mass ppm O (symbol 'A' in Figure 3). The deoxidation products mainly consisted of Al_2O_3 (red area) and Ti_3O_5 (yellow area) on the α-BCC matrix of Fe-Cr alloy (Figure 4(b)). The extracted oxide inclusions dispersed in the sample 'A' were also identified as Ti oxide (Figure 5(a)), Ti-rich TiO_x-Al_2O_3 inclusion (Figure 5(b)), and Al_2O_3 (Figure 5(c)). Since the observed inclusions were mostly pure alumina and Ti oxide, the predominance diagram calculated under the unit activity of the oxide phases (Figure 3) is valid. However, further research is required to describe the small solubility of Al in the Ti_3O_5 solid solution of the pseudobrookite structure. It can be concluded that the Fe-Cr alloy melt is in equilibrium with pure Al_2O_3 and Ti_3O_5 simultaneously by the complex deoxidation. No solid Al_2TiO_5 or liquid oxide phases were observed from the formed oxide layer and the extracted inclusions under the present experimental condition.

IV. CONCLUSIONS

In the present study, the deoxidation equilibria in the Fe-Cr-Al-O, Fe-Cr-Ti-O, and Fe-Cr-Al-Ti-O alloy melts were measured and thermodynamically analyzed over the wide range of Cr concentration up to 19.6 mass pct Cr at 1823 K to 1923 K (1550 °C to 1650 °C). The reliable thermodynamic data of the interaction parameters and the Gibbs free energies of the oxide formation were selected for reproducing the deoxidation results in the Fe-Cr-Al-O and Fe-Cr-Ti-O systems. In the Fe-Cr-Al-Ti-O system, the complex deoxidation experiments were carried out by the simultaneous addition of Al and Ti in Fe-18 mass pct Cr melt under the co-saturation condition of Al_2O_3 and Ti_3O_5. The results were in good agreement with the inclusion predominance diagram constructed using the thermodynamic parameters selected for the multicomponent Fe-Cr-Al-Ti-O system. In the typical ferritic stainless steel composition, no solid Al_2TiO_5 or liquid oxide phases were observed.

REFERENCES

1. W. Gordon and A. van Bennekom: *Mater. Sci. Technol.*, 1996, vol. 12, pp. 126–31.
2. H. Matsuura, C. Wang, G. Wen, and S. Sridhar: *ISIJ Int.*, 2007, vol. 47, pp. 1265–74.
3. M.A. Van Ende, M. Guo, R. Dekkers, M. Burty, J. Van Dyck, P.T. Jones, B. Blanpain, and P. Wollants: *ISIJ Int.*, 2009, vol. 49, pp. 1133–40.
4. W.C. Doo, D.Y. Kim, S.C. Kang, and K.W. Yi: *Met. Mater. Int.*, 2007, vol. 13, pp. 249–55.
5. M.K. Sun, I.H. Jung, and H.G. Lee: *Met. Mater. Int.*, 2008, vol. 14, pp. 791–98.
6. C. Wang, N.T. Nuhfer, and S. Sridhar: *Metall. Mater. Trans. B*, 2009, vol. 40B, pp. 1005–21.
7. M. Kiviö and L. Holappa: *Metall. Mater. Trans. B*, 2012, vol. 43B, pp. 233–40.
8. T. Zhang, C. Liu, and M. Jiang: *Metall. Mater. Trans. B*, 2016, vol. 47B, pp. 2253–62.
9. W.Y. Kim, J.O. Jo, C.O. Lee, D.S. Kim, and J.J. Pak: *ISIJ Int.*, 2008, vol. 48, pp. 17–22.
10. I.H. Jung, G. Eriksson, P. Wu, and A. Pelton: *ISIJ Int.*, 2009, vol. 49, pp. 1290–97.
11. Y.B. Kang and S.H. Jung: *ISIJ Int.*, 2018, vol. 58, pp. 1371–82.
12. F. Ruby-Meyer, J. Lehmann, and H. Gaye: *Scand. J. Metall.*, 2000, vol. 29, pp. 206–12.

13. S. Basu, S.K. Choudhary, and N.U. Girase: *ISIJ Int.*, 2004, vol. 44, pp. 1653–60.
14. Y.B. Kang and J.H. Lee: *ISIJ Int.*, 2017, vol. 57, pp. 1665–67.
15. D.C. Park, I.H. Jung, P.C.H. Rhee, and H.G. Lee: *ISIJ Int.*, 2004, vol. 44, pp. 1669–78.
16. M. Kiviö, L. Holappa, and T. Iung: *Metall. Mater. Trans. B*, 2010, vol. 41B, pp. 1194–1204.
17. C. Wagner: *Thermodynamics of Alloys*, Addison-Wesley Press, Cambridge, MA, 1952, pp. 47–51.
18. M.K. Paek, J.J. Pak, and Y.B. Kang: *Metall. Trans. B*, 2015, vol. 46B (2015), pp. 2224–33.
19. M.K. Paek, J.M. Jang, H.J. Kang, and J.J. Pak: *ISIJ Int.*, 2013, vol. 53, pp. 535–37.
20. J.M. Jang, S.H. Seo, J.S. Han, D.S. Kim, Y.B. Kang, and J.J. Pak: *ISIJ Int.*, 2015, vol. 55, pp. 2318–24.
21. M.K. Paek, H.S. Son, J.M. Jang, and J.J. Pak: *ISIJ Int.*, 2020, vol. 60, pp. 640–48.
22. J.O. Jo, W.Y. Kim, C.O. Lee, and J.J. Pak: *ISIJ Int.*, 2010, vol. 50, pp. 1373–79.
23. J.J. Pak, J.O. Jo, S.I. Kim, W.Y. Kim, T.I. Chung, S.M. Seo, J.H. Park, and D.S. Kim: *ISIJ Int.*, 2007, vol. 47, pp. 16–24.
24. L.E. Rohde, A. Choudhury, and M. Wahlster: *Arch. Eisenhuttenwes.*, 1971, vol. 42, pp. 165–74.
25. H. Sakao and K. Sano: *J. Japan Inst. Metals*, 1959, vol. 23, pp. 671–74.
26. T. Itoh, T. Nagasaka, and M. Hino: *ISIJ Int.*, 2000, vol. 40, pp. 1051–58.
27. J.M. Jang, M.K. Paek, and J.J. Pak: *ISIJ Int.*, 2017, vol. 57, pp. 1821–30.
28. M.K. Paek, J.M. Jang, Y.B. Kang, and J.J. Pak: *Metall. Trans. B*, 2015, vol. 46B, pp. 1826–36.
29. Steelmaking Data Sourcebook: *The Japan Society for the Promotion of Science, The 19th Committee on Steelmaking*, Gordon and Breach Science Pub, New York, 1988.
30. Y. Nakamura and M. Uchimura: *Trans. Iron. Steel Inst. Jpn.*, 1973, vol. 13, pp. 343–49.
31. W.Y. Cha: Master's Thesis, Hanyang University, Korea, 2003.
32. S.J. Tae: Master's Thesis, Hanyang University, Korea, 2003.
33. J.H. Park, D.S. Kim, and S.B. Lee: *Metall. Trans. B*, 2005, vol. 36B, pp. 67–73.
34. H. Ohta and H. Suito: *ISIJ Int.*, 2003, vol. 43, pp. 1301–8.
35. A. McLean and H.B. Bell: *J. Iron Steel Inst.*, 1965, vol. 203, pp. 123–30.
36. T. Yoshikawa and K. Morita: *Metall. Mater. Trans. B*, 2007, vol. 38B, pp. 671–80.
37. S.H. Seok, T. Miki, and M. Hino: *ISIJ Int.*, 2009, vol. 49, pp. 1850–59.